A Fidelity Susceptibility Approach to Quantum Annealing of NP-hard problems

Jun Takahashi* and Koji Hukushima†
Department of Basic Science, University of Tokyo
3-8-1 Komaba, Meguro, Tokyo 153-8902, Japan
(Dated: December 28, 2016)

The computational complexity conjecture of NP $\not\subseteq$ BQP implies that there should be an exponentially small energy gap for Quantum Annealing (QA) of NP-hard problems. We aim to verify how this computation originated gapless point could be understood based on physics, using the quantum Monte Carlo method. As a result, we found a phase transition detectable only by the divergence of fidelity susceptibility. The exponentially small gapless points of each instance are all located in the phase found in this study, which suggests that this phase transition is the physical cause of the failure of QA for NP-hard problems.

PACS numbers: 03.67.Ac, 03.67.Lx, 64.70.Tg, 75.10.Nr

arXiv:1612.08554v1 [quant-ph] 27 Dec 2016

I. INTRODUCTION

Recent progress in quantum technology has greatly accelerated interests towards quantum computation. One of the promising techniques to use quantum effects for computation is Quantum Annealing (QA) [1–3]. QA uses quantum fluctuation induced by a Hamiltonian $\hat{H}_{\rm T}$, which is usually a simple transverse field $\sum_i \hat{\sigma}_i^x$. By constructing a problem Hamiltonian $\hat{H}_{\rm P}$, whose ground state encodes the answer of the problem in interest, the total Hamiltonian is

$$\hat{H}(\lambda) = (1-\lambda)\hat{H}_{\rm P} + \lambda \hat{H}_{\rm T}, \tag{1}$$

where the parameter λ is the time dependent control parameter. The sufficient condition of how slow the quantum fluctuation should be reduced is closely related to the minimum excitation gap $\Delta E_{\rm min}$ of $\hat{H}(\lambda)$. The quantum adiabatic theorem [4] guarantees that the quantum state starting from the ground state of $\hat{H}_{\rm T}$ will always remain in the instantaneous ground state with high probability, as long as λ is changed using time longer than $O(\Delta E_{\rm min}^{-2})$. Thus, for a fixed problem embedded in $\hat{H}_{\rm P}$, if there are only polynomially small energy gaps, it indicates that QA can solve the specific problem in polynomial time, which is considered as "efficient" in the computer science community [5, 6]. Early studies hinted polynomial time computation of NP-hard problems [7], however they turned out to be artifacts of finite-size effects [8]. After numerical supports that naive QA fails for NP-hard problems were found, some scenarios such as Anderson/many-body localization or spin glass transition [8–10] were proposed to explain the reason of this failure. The wide belief in the computer science community that even quantum computers would not be able to solve NP-hard problems in polynomial time (NP$\not\subseteq$BQP)[11], could be seen as a *computational complexity based* physical conjecture that says all $\hat{H}(\lambda)$ should have an exponentially small gapless point at some λ if $\hat{H}_{\rm P}$ corresponds to a NP-hard problem. Providing a physical picture to this conjecture would be of great importance for the understanding of the connection between computational complexity and physics. One of the convincing arguments was made using numerical approaches [12], showing that a fraction of samples exhibit first order phase transition-like behaviors in terms of the usual spin-glass order parameter q. Since first order transitions in quantum spin systems are usually accompanied with an exponentially small energy gap [13], they provide good reason that NP-hard problems could not be computed in polynomial time using QA. However, those first order transitions are strongly sample dependent, and no concrete arguments have been made for connecting the phenomena to the above mentioned scenarios.

In this work, we see if those "underlying phase transition" scenarios are correct at all, using quantum Monte-Carlo simulations. A natural strategy to see the underlying phase transition would be to take the sample average of the the spin-glass order parameter q which exhibited a first order transition-like behavior in individual samples. However, we find that this quantity does not exhibit any singularities when the sample average $\bar{q}$ is taken. This implies that another measure is necessary to see the phase transition in question, if it exists. We thus used the notion of *fidelity susceptibility* [14–16]. This quantity quantifies how rapid the ground state is changing in the λ direction. The fidelity susceptibility $\chi_{\rm F}$ is also proportional to the symmetric logarithmic derivative (SLD) Fisher information metric[17], and has been recently under interest for detecting phase transitions where the order parameter is unknown, such as topological order phases. Our work suggests that $\chi_{\rm F}$ is also useful for quantum spin-glass like models with quenched disorders.

By using stochastic series expansion (SSE), a variant of quantum Monte Carlo methods, we estimate the sample average of the fidelity susceptibility $\overline{\chi_{\rm F}}$. We show for a specific NP-hard problem that QA undergoes a phase transition at a certain value of λ. At this transition point, $\overline{\chi_{\rm F}}$ diverges, while other common quantities such as $\bar{q}$

* jt@huku.c.u-tokyo.ac.jp
† hukusima@phys.c.u-tokyo.ac.jp

does not show or has very weak singularity. This implies that although there is a quantum phase transition at the value of λ, the order parameter for this transition is yet unknown. However, since all of the first order like transitions occur at values below the transition point, this result suggests that the first order transitions could be understood as a phenomenon within a non-trivial quantum phase. The paper is organized as follows. First we explain our model, which is a specific NP-hard problem that we fix. Then we explain the numerical methods used in this work, together with how to measure the fidelity susceptibility $\chi_{\rm F}$ for this system. Section IV explains our main results, and finally we will conclude our work.

II. MODEL: MAXIMUM INDEPENDENT SET

We fix the NP-hard problem in consideration to the Maximum Independent Set (MIS) problem. This is the problem where given a graph $G = (V, E)$, one finds the maximum subset of vertices $I^* \subset V$ such that no two vertices in I^* are adjacent (i.e. $\forall i, j \in I^*, (i, j) \notin E$). Finding the solution of the MIS problem is equivalent to finding the ground state of a Hamiltonian with the Pauli matrix in the form of

$$\hat{H}_{\rm P} = \frac{c}{4} \sum_{(i,j)\in E} \hat{\sigma}_i^z \hat{\sigma}_j^z - \sum_i \frac{2 - cd_i}{4} \hat{\sigma}_i^z \tag{2}$$

where d_i is the degree of vertex i in graph G and we set $c > 1$ to be 2. We will generate random instances of the MIS problem by randomly generating the graph G in target. We first generate an Erdöes-Rényi random graph [18] and then randomly add extra edges to it in order to make the ground state unique. The details are explained in Appendix A. No degenerate ground state yields that the first excited gap ΔE surely determines the computation time. Another reason is that the first order transitions mentioned in the introduction are previously only observed in those examples which have unique solutions[12]. We should care that making the solution unique does not affect the *hardness* of the problem, and we describe the details of how this point is taken care of in Appendix B. We also confirm from [19] that the classical MIS of Erdös-Rényi random graphs with average degree $d > e = 2.718...$ is in the replica symmetry breaking (RSB) phase, and therefore use Erdös-Rényi random graphs with average degree $d = 3$ to start with. Adding edges to make the solution unique only effectively increases the average degree, and pushes the graph deeper into the RSB phase.

III. METHOD: SSE WITH REPLICA EXCHANGE AND FIDELITY SUSCEPTIBILITY

We adopt the SSE method for Ising spin systems [20, 21]. The SSE method effectively takes the Trotter limit in the path integral Monte Carlo method[22, 23], and is therefore free from systematic error caused by the Trotter decomposition. Assuming that the Hamiltonian $\hat{H}$ is decoupled into some local operators as $\hat{H} = -\sum_k \hat{W}_k$ and that with an appropriate basis $B = \{|\sigma_m\rangle\}_m$, the non-negative hopping elements $W_{k,m}$ for $\forall k, m$ are expressed as $\hat{W}_k|\sigma_m\rangle = W_{k,m}|\sigma_{m'}\rangle$ with $|\sigma_{m'}\rangle \in B$, the partition function Z is expanded as

$$Z := {\rm Tr}[e^{-\beta\hat{H}}] \tag{3}$$

$$= \sum_{n=0}^{\infty} \frac{\beta^n}{n!} \sum_{\{k_l\}} \sum_m \langle\sigma_m| \prod_{l=1}^{n} \hat{W}_{k_l} |\sigma_m\rangle. \tag{4}$$

SSE samples terms in the above summation using Markov chain Monte Carlo methods, by changing $|\sigma_m\rangle$, n and $\{\hat{W}_{k_l}\}_l$. For the present model, we take the z-basis for B and simply have every $(1-\lambda)J_{ij}\hat{\sigma}_i^z\hat{\sigma}_j^z$ terms, every $(1-\lambda)h_i\hat{\sigma}_i^z$ terms, and every $\lambda\hat{\sigma}_i^x$ terms as $\hat{W}_k$. By adding constants to each term, one could make all $W_{k,m} \geq 0$. We adopt the usual Swendsen–Wang type procedure for the global update, but with a minor modification due to the presence of local fields. We adjust the constant terms associated with the $(1-\lambda)h_i\hat{\sigma}_i^z$ terms, and make the corresponding $W_{k,m} = 0$ or $2(1-\lambda)h_i$. This allows us to treat those operators as same as other ones except for the global updates, where we never flip clusters which contain those operators.

Furthermore, we also adopt the exchange Monte Carlo method (EMC) to accelerate equilibration [24, 25]. We divide the parameter region $[\lambda_{\rm low}, \lambda_{\rm high}]$ into $R-1$ equidistributed intervals, and run R different SSE simulations with corresponding λ_r. Configurations of adjacent λ_r are exchanged with probability

$$\min\left[1,\ \left(\frac{\lambda_r}{\lambda_{r+1}}\right)^{T_{r+1}-T_r} \left(\frac{1-\lambda_r}{1-\lambda_{r+1}}\right)^{P_{r+1}-P_r}\right],$$

where T_r and P_r denote the number of operators coming from $\hat{H}_{\rm T}$ and $\hat{H}_{\rm P}$, respectively. This ensures that the over-all R runs will satisfy the detailed balance condition, resulting in acceleration of equilibration.

Since we take the strategy of observing the ground-state properties by sampling the equilibrium state with high enough β, we should extend the definition of fidelity to finite-temperature states as in [26],

$$F(\lambda, \lambda+\epsilon) = \sqrt{\frac{{\rm Tr}[e^{-\beta\hat{H}(\lambda)/2} e^{-\beta\hat{H}(\lambda+\epsilon)/2}]}{({\rm Tr}[e^{-\beta\hat{H}(\lambda)}]{\rm Tr}[e^{-\beta\hat{H}(\lambda+\epsilon)}])^{1/2}}}. \tag{5}$$

By expanding Eq. (5) up to the second term in ϵ, we obtain the representation of $\chi_{\rm F}$ for finite temperature as

$$\chi_{\rm F}^{T\neq 0} = \frac{\langle k_L k_R\rangle - \langle k_L\rangle\langle k_R\rangle}{2\lambda^2} + \frac{\langle l_L l_R\rangle - \langle l_L\rangle\langle l_R\rangle}{2(1-\lambda)^2} - \frac{\langle k_L l_R\rangle - \langle k_L\rangle\langle l_R\rangle}{2\lambda(1-\lambda)} - \frac{\langle l_L k_R\rangle - \langle l_L\rangle\langle k_R\rangle}{2\lambda(1-\lambda)}, \tag{6}$$

where k and l denote the number of operators within $\{\hat{W}_{k_l}\}_{l=1}^{n}$ coming from $\hat{H}_{\rm T}$, and $\hat{H}_{\rm P}$, respectively, and $\langle\cdots\rangle$ represents the Monte Carlo average. The subindices L and R represent the number of the according operators in the left half or the right half of the operator string $\{\hat{W}_{k_l}\}_{l=1}^{n}$. The center of the string is determined probabilistically for every sampled configuration, according to the binomial distribution among the possible $n+1$ points of division.

IV. NUMERICAL RESULTS

By using the SSE method together with EMC, we sample the equilibrium state of $\beta = 3.5N$ with N being the number of vertices of the problem. It is known that whenever $\beta > \Delta E_{\rm min}^{-1}$, the equilibrium state is close to the ground state [12, 27]. By fixing the system size N and increasing β, we see that usual observables saturate around $\beta \sim 1.5N$ and $\overline{\chi_{\rm F}}$ also saturates at $\beta \sim 3.5N$. Thus, sampling the thermal equilibrium state at $\beta = 3.5N$ is sufficient to see the properties of the ground state. 3072 samples were taken for system sizes $N = 20$ and 30, and 1.6×10^5 to 1.28×10^6 MCS to measure the quantities after the same amount for equilibration. In the following, we show 256 samples with $N = 50$ since they exhibit clearer first order transitions, but will not use them for sample averages due to lack of enough samples.

A. Spin-glass order parameter q

The spin-glass order parameter q (the overlap parameter) is defined as

$$q := \frac{1}{N}\sum_i \langle \hat{\sigma}_i^{(1)} \hat{\sigma}_i^{(2)} \rangle = \frac{1}{N}\sum_i \langle \hat{\sigma}_i \rangle^2, \qquad (7)$$

where the upper suffixes (1) and (2) are the labels for two independent systems with the same quenched disorder. In previous study [12], some samples of NP-hard problems exhibited an acute increase in q after a characteristic dip with decreasing λ and this phenomena was called first order phase transitions after a physical argument. First order phase transitions are notions which are well-defined only in the thermodynamic limit, however we will abuse the term in this paper following Ref. [12]. These first order transitions are also found in our model as in Fig. 1, and we confirmed that double peaks in the histogram of q and $F_{\rm ans}$ defined below were observed in the "transition points" of those "first order transitions", supporting the argument of Ref. [12].

The transition points and even the presence of the first order transitions are sample dependent. When we take the sample average of q to see the behavior of the ensemble as in Fig. 1 (inset), we are unable to see any size dependence nor singularities. The derivative with respect to λ, $\partial q/\partial\lambda$, also seems to have no singularities as seen in

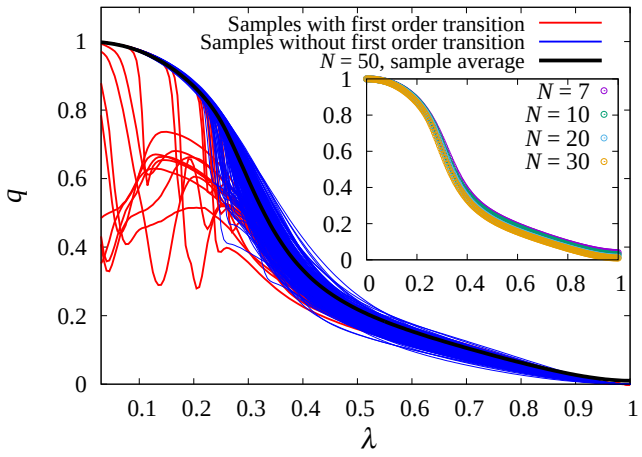

FIG. 1. The overlap parameter q is drawn as a function of λ for 256 samples with $N = 50$. Samples with dips are drawn in red, and samples without dips are in blue. The black line is the sample average $\bar{q}$. The inset presents $\bar{q}$ for different sizes.

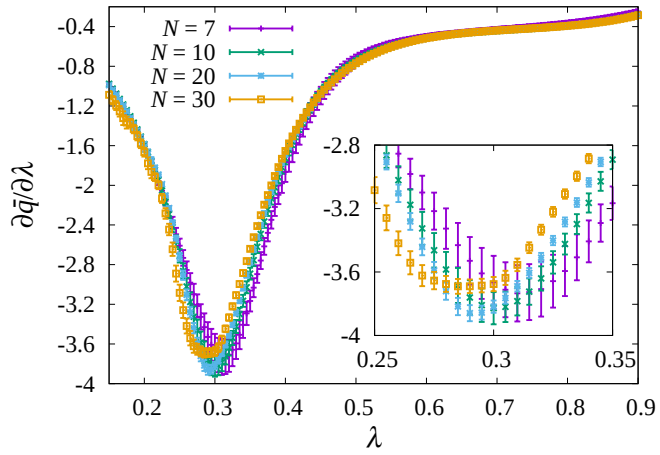

FIG. 2. The λ derivative of the averaged spin-glass order parameter $\bar{q}$ for different sizes are drawn for different sizes. The inset is a magnified view at the minimum point.

Fig. 2. This implies that although q was a good quantity for detecting first order phase transitions for individual samples in QA, it does not capture the underlying phase transition for this problem.

B. Fidelity susceptibility $\chi_{\rm F}$

Fig. 3 presents λ dependence of the fidelity susceptibility χ_F for each sample with $N = 50$. Similarly to q, $\chi_{\rm F}$ also shows an acute peak at the points where first order transitions occur (See Fig. 3). Other than the acute peaks corresponding to the first order transitions, we can see a relatively moderate peak at $\lambda \sim 0.3$. Importantly, this moderate peak is present in samples of both types,

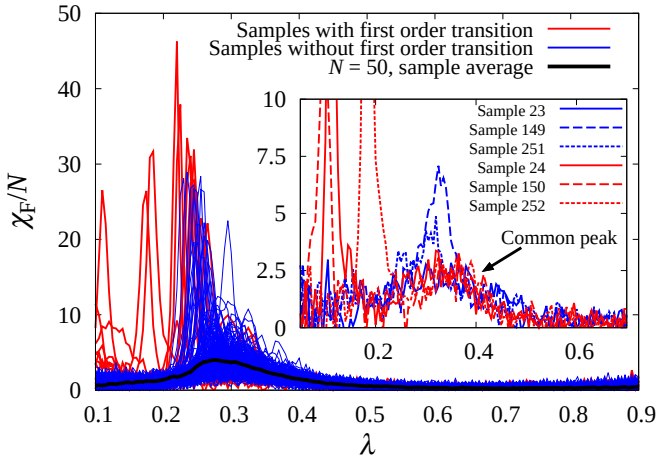

FIG. 3. λ dependence of the fidelity susceptibility $\chi_{\rm F}$ for 256 samples with $N = 50$. The use of colors is the same as Fig. 1. The inset shows a magnified view of 6 samples for clarity. The arrow is pointing at the moderate peak of $\chi_{\rm F}$ at $\lambda \sim 0.3$

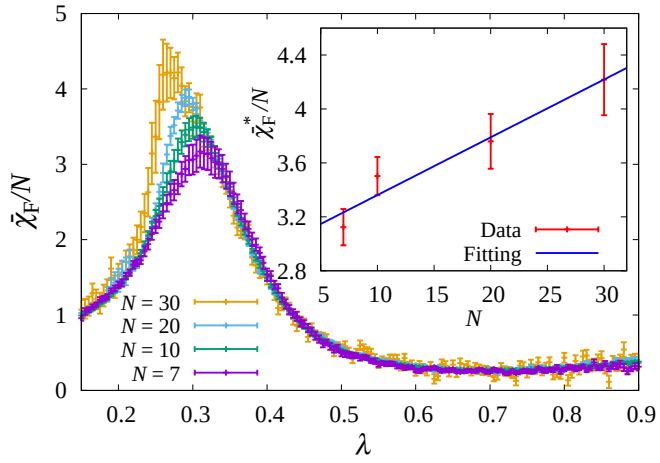

FIG. 4. The sample average of normalized fidelity susceptibility $\overline{\chi_{\rm F}}/N$ is drawn for different system sizes. The inset shows peak values and a least square fitting.

either with or without first order transitions, as seen in the inset of Fig. 3. This indicates that there may be a phase transition which is different from the first order transitions previously discussed.

To see this more clearly, the sample average of the fidelity susceptibility $\overline{\chi_{\rm F}}$ is taken in Fig. 4. It shows a diverging trend towards the thermodynamic limit. It should be noted that all of the first order transitions occur within the low λ phase of this transition, which indicates that this phase causes the first order transitions.

We do not understand yet what type of phase transitions this is, since they do not accompany any singularities in either q, nor $S_{\rm ans}$, a Rényi entropy-like quantity which will be explained in the following section.

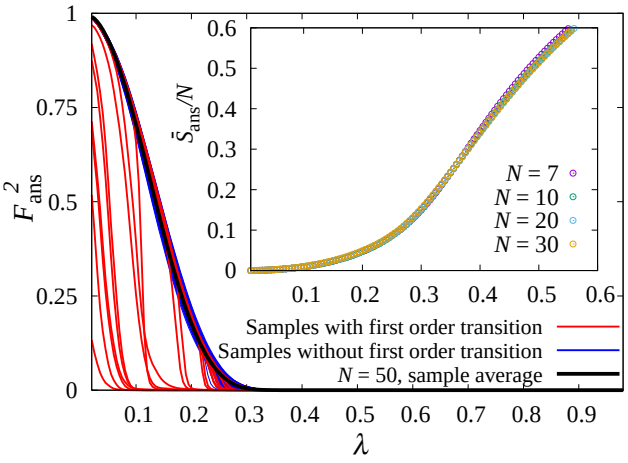

FIG. 5. Square of the answer fidelity $F_{\rm ans}^2 = \langle \hat{P}_{\rm ans} \rangle$ for 256 samples with $N = 50$. The inset shows the sample average of $-\log_2\langle \hat{P}_{\rm ans}\rangle/N$, i.e. $\overline{S_{\rm ans}}/N$ for different sizes.

C. Answer Fidelity

We can easily measure the fidelity between the ground state of a particular λ and that of $\lambda = 0$, since we make the solution of MIS unique. We will call this as the answer fidelity $F_{\rm ans} := F(\lambda, 0)$, and this will represent the (square root of) the probability of observing the correct answer by a projection measurement with the z-basis, $\langle \hat{P}_{\rm ans} \rangle$.

Since the answer fidelity is 0 for $\lambda = 1$ in the thermodynamic limit and it takes 1 for $\lambda = 0$, it could be a natural candidate for an order parameter. Indeed, as we can see from Fig. 5, the answer fidelity jumps from almost 0 to a finite value in samples exhibiting first order transition. Also, samples without first order transitions also start to have non-negligible values from a certain value of λ. It is tempting to think that the phase transition captured by $\chi_{\rm F}$ is a transition from a $F_{\rm ans} = 0$ phase to a $F_{\rm ans} > 0$ phase, but is incorrect. This is because $F_{\rm ans}$ seems to converge to 0 for all $\lambda > 0$. In fact, If we plot $S_{\rm ans} := -\log_2\langle \hat{P}_{\rm ans}\rangle$ normalized by N, they collapse into a common curve as in the inset of Fig. 5. This is natural, since when λ is small enough and if $F_{\rm ans}$ is larger than the fidelity between the ground state and any other basis state of the z direction $|\boldsymbol{\sigma}\rangle$, $S_{\rm ans}$ is actually equivalent to the Rényi entropy [28, 29]

$$S_n(\lambda) := \frac{1}{1-n} \sum_{\boldsymbol{\sigma}} \left| \langle \boldsymbol{\sigma} | {\rm GS}(\lambda) \rangle \right|^{2n}, \tag{8}$$

in the $n \to \infty$ limit, where $|{\rm GS}(\lambda)\rangle$ is the ground state of $\hat{H}(\lambda)$. By assuming that S_∞/N converges to a finite value, and that $S_\infty = S_{\rm ans}$, it is easy to see that $F_{\rm ans}$ goes to 0 for all $\lambda > 0$. Similarly to q, although both $F_{\rm ans}$ or $S_{\rm ans}$ seems to capture the first order transitions, when we take the sample average of them, no singularities could be observed.

V. CONCLUSION AND DISCUSSIONS

We have demonstrated that the fidelity susceptibility can be useful to find quantum phase transitions which would otherwise have been hard to confirm. For the MIS with unique solutions, we find a divergence in $\overline{\chi_{\rm F}}$, which other conventional quantities fail to capture. Furthermore, previously known first order phase transitions in unique solution ensembles of NP hard problems occur in the low-λ side of this $\overline{\chi_{\rm F}}$ divergence. This implies that this ordered phase could be understood as the physical consequence of the computational complexity conjecture, however the connections to existing physical scenarios such as spin glass transitions, or Anderson/many-body localization are yet to be confirmed. Further examination of the divergence of $\chi_{\rm F}$, e.g. the critical exponent of $\chi_{\rm F}$ and its connections to other critical exponents, should be carried out for comparison of different scenarios.

It should be noted that even if quantities like q do not show singularities, it does not necessarily mean that the spin glass picture is wrong. For example, a continuous replica symmetry breaking picture would be compatible with no singularities in $\bar{q}$. However, to confirm that scenario, one would have to calculate the histogram $P(q)$ which is rather tedious. The fidelity susceptibility $\chi_{\rm F}$ provides an easier way to confirm the existence of a subtle quantum phase transition. Consistencies with known freezing phenomena found in the actual quantum annealing machine [30] is also an interesting and important problem.

We emphasize that $\chi_{\rm F}$ also shows a very sharp peak at the first order transitions which occur within the low λ side of the phase transition. This suggests that $\chi_{\rm F}$ may actually detect all of the transitions which is relevant for QA. Previous results [26] show that $\chi_{\rm F}$ could be used as indicators for various transitions including spin liquids etc. The present work shows that it is also true for the case of QA of NP-hard problems which is glassy and has quenched disorders.

ACKNOWLEDGMENTS

We thank Y. Nishikawa for useful discussions. Numerical simulation in this work has mainly been performed by using the facility of the Supercomputer Center, Institute for Solid State Physics, the University of Tokyo. This research was supported by the Grants-in-Aid for Scientific Research from the JSPS, Japan (No. 25120010 and 25610102).

Appendix A: The Unique solution ensemble

Instead of using simple Erdös-Rényi random graphs which have multiple solutions for the MIS, we use random graphs which have unique solutions. This ensures that it is always the minimum energy gap $\Delta E_{\rm min}$ that causes the failure of QA. If there are multiple solutions, a small $\Delta E_{\rm min}$ would not necessarily imply failure, since it can still end in the degenerate ground state of $\hat{H}_{\rm P}$. To generate random-graph ensemble with a unique solution, we randomly add edges to the Erdös-Rényi random graph in the following way. If the original Erdös-Rényi random graph already has a unique solution, we can just use it, although the probability of such a graph occurring decreases as N increases. When the graph has multiple solutions, it means the vertices could be divided into two groups, namely the backbones and the non-backbones. The backbones are the vertices which are constantly in the independent set or out of it through out all the possible solutions. If a given graph has a unique solution, all the vertices belong to the backbone by definition. After checking which vertices the backbones are, we randomly assign one of the possible solutions, at random. If there are more than two non-backbones which are inside of the assigned solution, we add an edge between those two vertices. This makes the chosen solution no longer valid, while making sure that there are still solutions of the same size. We continue this process until there are no more pairs of non-backbones inside a particular maximum independent set solution. If there still remains a non-backbone vertex with no pair, we randomly choose one backbone vertex within the solution and add an edge with that. This procedure always decreases the degeneracy. When the degeneracy is totally removed and the solution is unique, the procedure ends successfully. If feasible solutions vanish during this procedure, we discard the graph and start all over again. We call this stochastically generated ensemble of graphs, the unique solution ensemble in this paper.

Appendix B: The Dynamic Programming Leaf Removal Algorithm

We should confirm that the process of making the solution unique does not make the problem easier, since we want to know the physical picture of *hard* problems. A specific algorithm which we call the Dynamic Programming Leaf Removal algorithm (DPLR) was used for confirming this point. DPLR is a combination of leaf removal(LR)[31], a standard algorithm for MIS, and dynamic programming, a well known algorithmic technique.

The LR algorithm is described in Table I. We set $k = 0$ and $S_v \equiv 0$ for the input. They will serve as intermediate memories during the recursion of DPLR. k represents the largest independent set found so far, and S_v represents the configuration corresponding to that. The LR algorithm only runs until it hits a "core" where there are no longer vertices with degree less than 2.

We modify the LR algorithm by making leaves, which are vertices with degree below 2, with setting a random vertex to be either in the independent set or not and compare the two results recursively. The algorithm is presented in Table II. Again, we set $k = 0$ and $S_v \equiv 0$ for

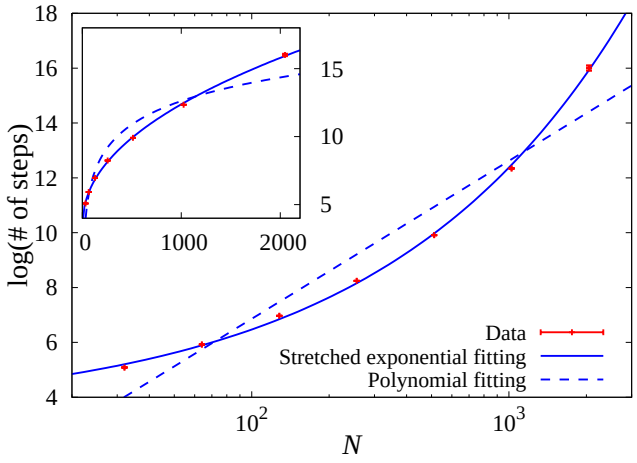

FIG. 6. The logarithm of median time steps needed to find the MIS for Erdös-Rényi random graphs using the DPLR algorithm is shown as a function of the system size N. The inset shows the same plot with non-logarithmic scale for the horizontal axis. All lines are obtained by least square fittings, either assuming $y = aN^b + c$ (stretched exponential) or $y = c + d\log(N)$ (polynomial). The stretched exponent b is estimated as $b = 0.465(25)$.

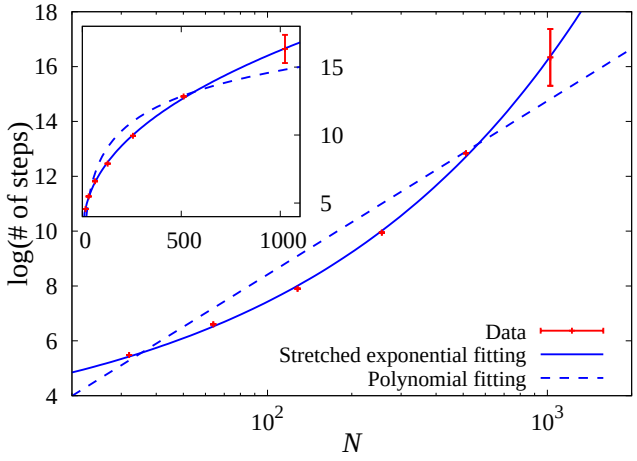

FIG. 7. The logarithm of median time steps needed to find the MIS for randomly generated unique solution graphs, using the DPLR algorithm. The inset shows the same plot with non-logarithmic scale for the horizontal axis. The fittings are performed as the same as in Fig. 6, yielding that the stretched exponent $b = 0.433(19)$.

the original input. k in the final output will represent the size of the maximum independent set, and S_v in the final output will represent the corresponding configuration.

It should be noted that this DPLR algorithm is the analogue of the well-known DPLL algorithm[32] for the satisfiability problem. As it is known that the running time of DPLL scales polynomially in the easy parameter region of SAT[33], DPLR should be a fairly good algorithm to see the hardness of the MIS problem.

Algorithm 1 LR

Input $(G = (V, E), \{S_v\}, k)$
while there exist a vertex v with $S_v = 0$ and degree< 2 **do**
  $k++$
  if degree of $v = 0$ **then**
    set $S_v = 1$
    remove v from the graph G
  end if
  if degree of $v = 1$ **then**
    set $S_v = 1$
    for the vertex w adjacent to v, set $S_w = -1$
    remove v and w from graph G
  end if
end while
return $(G, \{S_v\}, k)$

TABLE I. Pseudo code of the LR algorithm.

Algorithm 2 DPLR

Input $(G = (V, E), \{S_v\}, k)$
$(G, \{S_v\}, k) \leftarrow \mathrm{LR}(G, \{S_v\}, k)$
if $V \neq \varnothing$ **then**
  choose one vertex from the remaining graph $v \in V$
  $(G', \{S'_v\}, k') \leftarrow \mathrm{DPLR}(\mathrm{INC}(G, v), \{S_v\}, k)$
  $(G'', \{S''_v\}, k'') \leftarrow \mathrm{DPLR}(\mathrm{EXC}(G, v), \{S_v\}, k)$
  if $k' + 1 \geq k''$ **then**
    return $(G', \{S'_v\}, k' + 1)$
  else
    return $(G'', \{S''_v\}, k'')$
  end if
else
  return $(G, \{S_v\}, k)$
end if
function INC$(G = (V, E), v)$
  remove v and adjacent vertices $w \in \partial v$ from graph G
  return G
end function
function EXC$(G = (V, E), v)$
  remove v from graph G
  return G
end function

TABLE II. Pseudo code of the DPLR algorithm.

We can compare the simple Erdös-Rényi random graphs and the unique solution ensemble in terms of computation time using DPLR, from Fig. 6 and Fig. 7. Since the distribution of time steps has exponentially long tails, it is convenient to focus on the logarithm of the time steps needed. We plot the logarithm of the median time steps needed for finding and confirming a solution for the MIS problem. We used over 1000 samples for each sizes to estimate the median value, and the error bars are drawn by the bootstrap method. Calculating by the logarithm

of the time step allows us to have small error bars, which otherwise would require an exponential amount of data to have constant size error bars. Importantly, the median time step shows stretched exponential scaling for both ensembles. We can see that a polynomial scaling, shown by the dotted lines in Fig. 6 and Fig. 7, does not fit, and a stretched exponential scaling does. The fact that the median computation time grows stretched exponentially implies that at least half of the samples will be hard instances. The exponents are $N^{0.465\pm0.025}$ and $N^{0.433\pm0.019}$ for Erdös-Rényi random graphs and the unique solution ensemble respectively. The fact that both ensembles scale stretched exponentially and not polynomially implies that the MIS problem is hard for both ensembles and we have not changed the hardness of the problem drastically by making the solution unique described in Appendix A.

[1] T. Kadowaki and H. Nishimori, Phys. Rev. E **58**, 5355 (1998).
[2] E. Farhi, J. Goldstone, S. Gutmann, and M. Sipser, arXiv:quant-ph , 0001106 (2000).
[3] S. Boixo, T. F. Rønnow, S. V. Isakov, Z. Wang, D. Wecker, D. A. Lidar, J. M. Martinis, and M. Troyer, Nat. Phys. **10**, 218 (2014).
[4] T. Kato, J. Phys. Soc. Jpn. **5**, 435 (1950).
[5] S. Arora and B. Barak, *Computational Complexity: A Modern Approach* (Cambridge University Press, 2009).
[6] C. Moore and S. Mertens, *The Nature of Computation* (Oxford Univ Press, 2011).
[7] E. Farhi, J. Goldstone, S. Gutmann, J. Lapan, A. Lundgren, and D. Preda, Science **292**, 472 (2001).
[8] V. Bapst, L. Foini, F. Krzakala, G. Semerjian, and F. Zamponi, Phys. Rep. **523**, 127 (2013).
[9] M. H. S. Amin and V. Choi, Phys. Rev. A **80**, 062326 (2009).
[10] B. Altshuler, H. Krovi, and J. Roland, Proc. Natl Acad. Sci. USA **107**, 12446 (2010).
[11] C. H. Bennett, E. Bernstein, G. Brassard, and U. Vazirani, SIAM J. Comput. **26**, 1510 (1997).
[12] A. P. Young, S. Kynsh, and V. N. Smelyanskiy, Phys. Rev. Lett. **104**, 020502 (2010).
[13] V. Bapst and G. Semerjian, J. Stat. Mech. **2012**, 06007 (2012).
[14] W. L. You, Y. W. Li, and S. J. Gu, Phys. Rev. E **76**, 022101 (2007).
[15] S. J. Gu, Int. J. Mod. Phys. B. **24**, 4371 (2010).
[16] S. Garnerone, N. T. Jacobson, S. Haas, and P. Zanardi, Phys. Rev. Lett. **102**, 057205 (2009).
[17] A. Fujiwara and H. Nagaoka, Phys. Lett. A **201**, 119 (1995).
[18] P. Erdös and A. Rényi, Publicationes Mathematicae **6**, 290 (1959).
[19] H. Zhou, Eur. Phys. J. B **32**, 265 (2003).
[20] A. W. Sandvik, Phys. Rev. E **68**, 056701 (2003).
[21] A. W. Sandvik, Phys. Rev. B **59**, 14157 (1999).
[22] M. Suzuki, Progr. Theo. Phys. **56**, 1454 (1976).
[23] H. F. Trotter, Proc. Am. Math. Soc. **19**, 545 (1959).
[24] K. Hukushima and K. Nemoto, J. Phys. Soc. Jpn. **65**, 1604 (1996).
[25] I. Hen and A. P. Young, Phys. Rev. E **84**, 061152 (2011).
[26] L. Wang, Y.-H. Liu, J. Imriška, P. N. Ma, and M. Troyer, Phys. Rev. X **5**, 031007 (2015).
[27] S. Yasuda, H. Suwa, and S. Todo, Phys. Rev. B **92**, 104411 (2015).
[28] A. Rényi, Proc. Fourth Berkeley Symp. on Math. Statist. and Prob. **1**, 547 (1961).
[29] F. Franchini, A. R. Its, and V. E. Korepin, J. Phys. A. **41**, 025302 (2008).
[30] M. H. S. Amin, Phys. Rev. A **92**, 052323 (2015).
[31] M. Bauer and O. Golinelli, Eur. Phys. J. B **24**, 339 (2001).
[32] M. Davis and H. Putnam, J. Symb. Logic **31**, 125 (1966).
[33] B. Selman and S. Kirkpatrick, Artif. Intell. **81**, 273 (1996).